The cause of negative CO2 forcing at the top-of-atmosphere: the role of stratospheric vs. tropospheric temperature inversions

Yan-Ting Chen[1], Timothy Merlis[2], and Yi Huang[1]

[1]McGill University
[2]Princeton University

September 28, 2023

Abstract

Increasing carbon dioxide (CO2) in the atmosphere usually reduces Earth's outgoing longwave radiation (OLR). The unusual case of Antarctica, where CO2 enhances OLR and implies a negative forcing, has previously been explained by the strong near-surface inversion or extremely low surface temperature. However, negative forcing can occasionally be found in the Arctic and tropics where neither of these explanations applies. Here, we examine the changes in infrared opacity from CO2 doubling in these low or negative forcing climate states, which shows the predominant role of the stratospheric contribution to the broadband forcing. Negative forcing in today's climate demands a combination of strong negative forcing caused by a steep stratospheric temperature inversion and a weaker positive forcing in the atmospheric window, which can be caused by a low surface temperature or a strong high cloud masking effect. Contrary to conventional wisdom, the near-surface inversion has little impact on the forcing.

The cause of negative CO_2 forcing at the top-of-atmosphere: the role of stratospheric vs. tropospheric temperature inversions

Yan-Ting Chen[1], Timothy M. Merlis[2], and Yi Huang[1]

[1]Department of Atmospheric and Oceanic Sciences, McGill University, Montreal, Quebec, Canada
[2]Program in Atmospheric and Oceanic Sciences, Princeton University, Princeton, NJ, USA

Key Points:

- In addition to Antarctica, increased CO_2 increases OLR in the Arctic and deep tropics under certain circumstances.
- In polar regions, negative CO_2 forcing arises from stratospheric temperature inversions, while near-surface inversions have a small effect.
- CO_2 forcing can be negative in other regions when the high clouds block the tropospheric emission, leaving the stratospheric contribution.

Corresponding author: Yan-Ting Chen, `yan-ting.chen@mail.mcgill.ca`

Abstract

Increasing carbon dioxide (CO_2) in the atmosphere usually reduces Earth's outgoing longwave radiation (OLR). The unusual case of Antarctica, where CO_2 enhances OLR and implies a negative forcing, has previously been explained by the strong near-surface inversion or extremely low surface temperature. However, negative forcing can occasionally be found in the Arctic and tropics where neither of these explanations applies. Here, we examine the changes in infrared opacity from CO_2 doubling in these low or negative forcing climate states, which shows the predominant role of the stratospheric contribution to the broadband forcing. Negative forcing in today's climate demands a combination of strong negative forcing caused by a steep stratospheric temperature inversion and a weaker positive forcing in the atmospheric window, which can be caused by a low surface temperature or a strong high cloud masking effect. Contrary to conventional wisdom, the near-surface inversion has little impact on the forcing.

Plain Language Summary

CO_2, as an important greenhouse gas, is known to reduce the Earth's longwave emission, provoking a positive forcing that increases the net flow of energy into the Earth system. In this study, we discuss the cause of negative forcing, where CO_2 increases longwave emission that happens most commonly in Antarctica and in some rare conditions in the Arctic and tropics. In contrast to conventional arguments that a near-surface temperature increase with altitude is key to a negative forcing, we show that the stratospheric temperature and, in the tropics, clouds play a more important role. The results are based on temperature modification experiments and an analysis of the vertical structure of atmospheric emission changes. While a negative forcing does not mean the surface would cool since there are other important adjustments involved in the re-establishment of energy balance, the results show the values of resolving the spectral dimension of radiation to quantify the radiative sensitivity to the near-surface and stratosphere temperature structure.

1 Introduction

It is known that increasing carbon dioxide (CO_2) concentration enhances the greenhouse effect and results in positive longwave radiative forcing at the top-of-atmosphere (TOA), leading to an increase in Earth's radiation budget. While this is true in general, it has also been shown that the CO_2 forcing can enhance longwave emission-to-space in Antarctica, which is a negative TOA forcing. Such phenomenon is found in radiative transfer calculations (Zhang & Huang, 2014; Flanner et al., 2018; Jeevanjee et al., 2021; Freese & Cronin, 2021; Chen et al., 2023) and climate models (Schmithüsen et al., 2015; Huang et al., 2016; Smith et al., 2018), with support from observations (Schmithüsen et al., 2015; Sejas et al., 2018). Although a negative TOA forcing there might not translate to surface cooling (Smith et al., 2018; Freese & Cronin, 2021), understanding what distinguishes the radiative forcing in Antarctica from other parts of the climate helps improve theoretical understanding of the radiative forcing.

Existing understandings from spectral radiative transfer properties sheds light on negative TOA forcing from increased CO_2. This can result from the non-monotonic vertical temperature structure. In a non-scattering atmosphere, the radiative fluxes at the TOA ($z = \infty$) at a wavenumber ν can be written as:

$$I_\nu(\infty) = B_\nu(0)\,Tr_\nu(0) + \int_0^\infty B_\nu(z)\,W_\nu(z)\,dz, \tag{1}$$

$$Tr_\nu(z) \equiv e^{-\tau_\nu(z)}, \tag{2}$$

$$W_\nu(z) \equiv \frac{dTr_\nu(z)}{dz}, \tag{3}$$

where I_ν is the monochromatic radiance, $B_\nu(z)$ is the thermal emission of the layer at the height z, $Tr_\nu(z)$ is the transmissivity between z and the TOA. $\tau_\nu(z)$ is the optical depth between the TOA and z that monotonically increases from the TOA to the surface, and $W_\nu(z)$, the weighting function, is the derivative of the transmission function with height.

As CO_2 increases, the altitude of the weighting function peak, or the so-called emission layer where $\tau_\nu(z) = 1$, shifts to a higher level (e.g., Huang & Bani Shahabadi, 2014). When collocated with a temperature inversion, the elevated emission layer enhances emission-to-space from the warmer air (as opposed to having colder air above, as is typical in the troposphere) and therefore leads to a negative TOA forcing. Such negative forcing in monochromatic radiance has been identified in individual wavelengths where the emission layer shifts within either stratospheric (Huang & Bani Shahabadi, 2014) or near-surface (Flanner et al., 2018; Sejas et al., 2018) temperature inversion. As the gas absorption properties vary spectrally, the behavior at a single wavelength does not determine the broadband results. Antarctica, interestingly, is a region where the negative forcing remains after spectral integration.

From a simplified, broadband perspective, Schmithüsen et al. (2015) and Smith et al. (2018) approximated the TOA forcing with a two-level model. Assuming an effective emission temperature of the atmosphere and the Earth's surface is a blackbody, the outgoing longwave radiation (OLR) at the TOA is expressed as:

$$\text{OLR} = (1 - \epsilon_{ATM})\sigma T_{SFC}^4 + \epsilon_{ATM}\sigma T_{ATM}^4, \tag{4}$$

where ϵ_{ATM} is the broadband emissivity of the atmosphere and equals broadband $1 - Tr(0)$ in (1). As higher CO_2 concentration increases ϵ_{ATM}, the dependency of instantaneous forcing is then:

$$\frac{\partial \text{OLR}}{\partial \epsilon_{ATM}} = \sigma(T_{ATM}^4 - T_{SFC}^4). \tag{5}$$

From this equation, the sign of the forcing is determined by the temperature contrast between the surface and the atmosphere: when $T_{ATM} > T_{SFC}$, OLR increases as CO_2 increases ϵ_{ATM}. Negative forcing in Antarctica is then explained by the fact that T_{SFC} in Antarctica is lower than the lower troposphere (owing to near-surface inversion) or the stratosphere. This explanation partly echoes the emission layer-based argument that the air temperature structure is important for the forcing, but T_{ATM} in (5) is not clearly defined and itself could be a function of CO_2 concentration. Moreover, the forcing caused by ϵ_{ATM} change is found positive even in Antarctica [blue dots in Figs. 9f,h of Chen et al. (2023)]. The utility of the broadband analytical model and the role of near-surface versus the stratospheric temperature structure, therefore, remains obscure.

Negative TOA forcing also happens outside of Antarctica. The Arctic sometimes exhibits strong negative forcing (Fig. 1a). Negative forcing even occurs in the tropics and mid-latitudes for instances of strong longwave cloud radiative effects (CRE), when the all-sky OLR is much lower than the clear-sky OLR. Although such extreme events are smoothed out in the long-term average, these occasions of negative forcing are worth documenting and suggest that there are other factors that can sharply modify the forcing, in addition to simple surface temperature-based or stratospheric temperature-based arguments.

This study explores the causes of negative TOA CO_2 forcing in the polar regions and tropics. The distinct climates there will generalize the current understanding of how the temperature structure and clouds shape the instantaneous CO_2 forcing at the TOA. The radiative transfer model and the dataset used here are described in Section 2. In section 3, we focus on the causes of negative forcing under clear-sky conditions, which

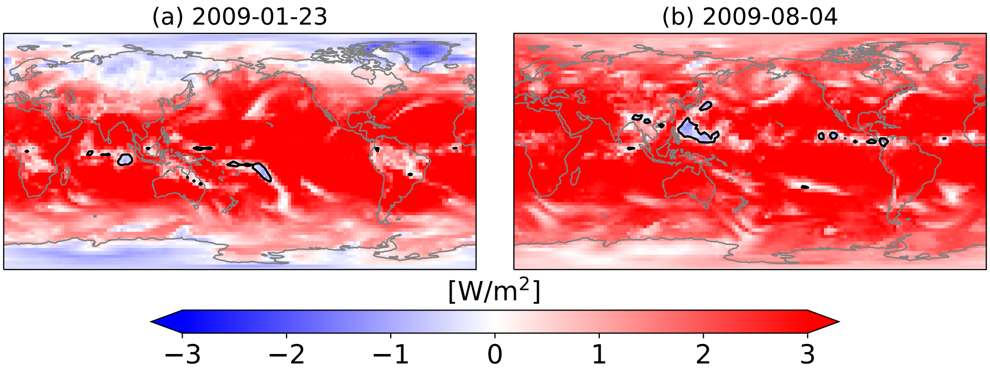

Figure 1. The daily-mean forcing pattern on (a) Jan 23, 2009, near the onset of a major mid-winter SSW event and (b) Aug 4, 2009, when there are strong cloud masking effects in the western North Pacific from intensifying typhoon Morakot. The black contour shows longwave cloud radiative effect (CRE) of $120\,\mathrm{Wm}^{-2}$.

mainly occurs in Antarctica. We quantify the forcing contributed by the near-surface temperature inversion and stratospheric inversion, with a novel approach that decomposes the forcing into bulk spectral regions, which feature different sensitivities to temperature structures. We also discuss why the negative CO_2 forcing is less common in the Arctic than Antarctica. Section 4 discusses negative forcing under all-sky conditions. We also use idealized experiments, in which the temperature and clouds are modified to show how the temperature structure and clouds affect the sign of CO_2 forcing. We conclude in section 5.

2 Radiative transfer calculation

We use standalone longwave Rapid Radiative Transfer Model (RRTMG, Mlawer et al., 1997), which calculates fluxes ranging from $10\,\mathrm{cm}^{-1}$ to $3250\,\mathrm{cm}^{-1}$. The climatology of atmospheric profiles, including temperature, specific humidity, and ozone, are from ERA5 reanalysis dataset of the European Centre for Medium-Range Weather Forecasts (Hersbach et al., 2020). The radiative forcing of doubled CO_2 is calculated as the flux difference between 760 and 380 ppmv CO_2 concentrations. The concentration of other well-mixed greenhouse gases, CH_4 and N_2O, are prescribed to 1.797 and 0.323 ppmv, respectively. CFCs are not included.

RRTMG performs the radiative transfer calculation at a total of 140 g-points, with each accounting for one monochromatic spectral node where the wavenumbers with similar absorption coefficients are grouped together beforehand. The fluxes at individual g-points are summed to get the bandwise and the broadband fluxes. This technique, named the correlated-k method (Fu & Liou, 1992), is a numerical treatment that speeds up computation (vs. calculating fluxes at a small, fixed wavenumber increment like line-by-line radiative transfer).

3 Negative CO_2 forcing under clear-sky conditions

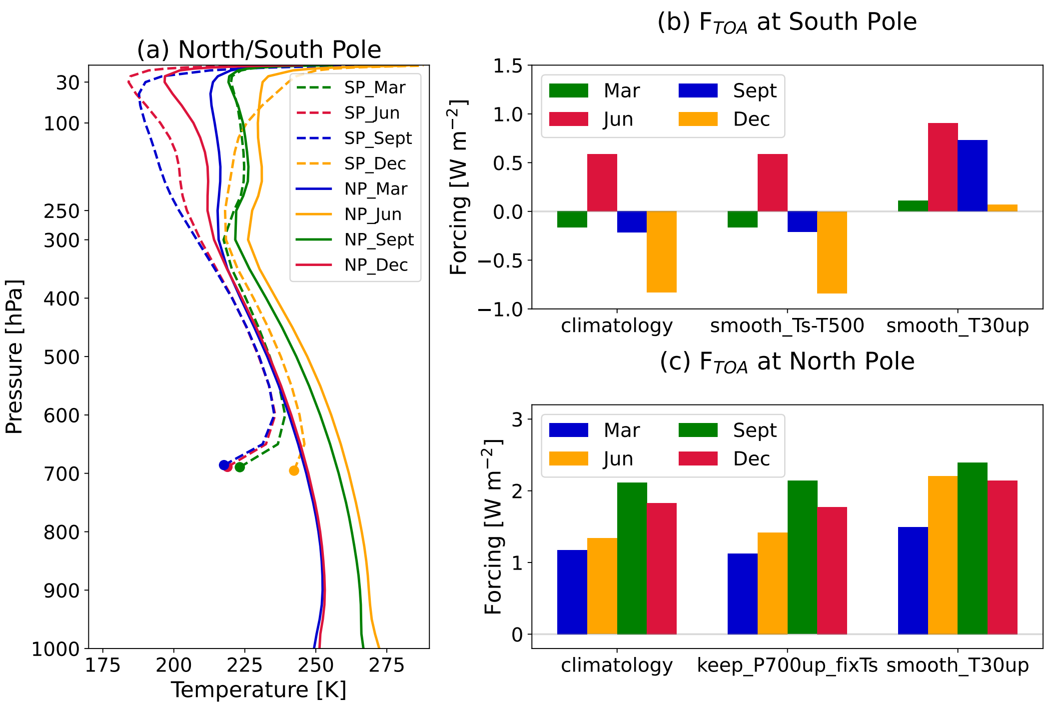

Figure 2. (a) The seasonality of climatological temperature at the South and North Pole. (b) The broadband, instantaneous CO_2 forcing at the TOA based on the climatological profile and temperature modification experiments of the South Pole (section 3.1). (c) Same as (b) but for the North Pole (section 3.3). Note that the range of y-axis in (b) and (c) is different.

3.1 Temperature modification experiments

To evaluate the role of inversions on CO_2 forcing, we calculate the forcing with modified temperature soundings of the South Pole. Specifically, the near-surface inversion is removed by replacing the temperature below 500 hPa with temperature at the 500 hPa (smooth_Ts-T500), and the stratospheric inversion is removed by setting temperature above 30 hPa with temperature at the 30 hPa (smooth_T30up). In both experiments, we choose to leave T_{SFC} unperturbed because T_{SFC} determines the upward longwave emission, which is an important energetic constraint. How T_{SFC} itself affects the forcing will be discussed at the end of this section. The water vapor in the polar regions is scarce and does not change the results qualitatively, so we keep using climatological water vapor profiles to highlight the role of temperature structure even if the near-surface layer might be supersaturated when the near-surface temperature is reduced.

Figures 2a,b plot the climatological temperature profile at the South Pole and the resulting instantaneous CO_2 forcing. Consistent with previous literature, the CO_2 forcing is found negative throughout September to March (Schmithüsen et al., 2015; Smith et al., 2018; Freese & Cronin, 2021; Chen et al., 2023). We note that December features the strongest negative forcing yet the near-surface inversion is the weakest. Surprisingly, despite large temperature reductions imposed in smooth_Ts-T500 experiment sometimes exceeds 20 K in the lower troposphere, the forcing changes by less than $0.01\,\mathrm{Wm^{-2}}$. In contrast, the changes in the stratospheric lapse rate in smooth_T30up effectively eliminate the negative forcing and can increase the forcing by $\sim 1\,\mathrm{Wm^{-2}}$. These suggest a dominant role of stratospheric temperature in modifying the CO_2 forcing, at least when T_{SFC} remains unchanged.

3.2 Attributing the radiative forcing to the temperature profile

According to (1), the flux at the TOA comes from various altitudes of the atmosphere owing to the wavelength-varying $\tau_\nu(z)$ and $W_\nu(z)$ structure. In other words, one can relate the forcing and the contributing atmospheric level by calculating $W_\nu(z)$ in (3) once $\tau_\nu(z)$ is known.

We exploit the spectral information in the model by outputting the optical depth and radiative fluxes at all 140 g-points, and regroup the g-point-based fluxes according to which part of the atmosphere the climatological emission layer $[\tau_g(z) = 1]$ belongs to. The g-point-based fluxes are sorted into three groups with the following definitions:

- Stratosphere: g-points which $\tau_g(z_{250}) > 1$.
- Troposphere: g-points which $\tau_g(z_{250}) < 1$ and $\tau_g(z_{sfc}) > 1$.

- Window: g-points which $\tau_g(z_{sfc}) < 1$.

The subscript of z denotes the associated pressure level, and the tropopause is set at 250 hPa for convenience. In this definition, the first term on the RHS of (1), the forcing coming from the surface, is included in the window group. Together with (3), the g-point grouped weighting function is calculated as:

$$W_i(z) = \frac{1}{I(0)} \sum_{g=0}^{n} I_g(0) \cdot \frac{dTr_g(z)}{dz}, \tag{6}$$

where the subscript g denotes the fluxes in the g-point dimension and the sum is over the g-points where the emission layer lies in the atmospheric layer group i defined above. Compared to using RRTMG's 16-band outputs that are segregated by respective gas absorption properties beforehand, this method offers a finer view of what part of the atmospheric profile contributes to the radiative fluxes.

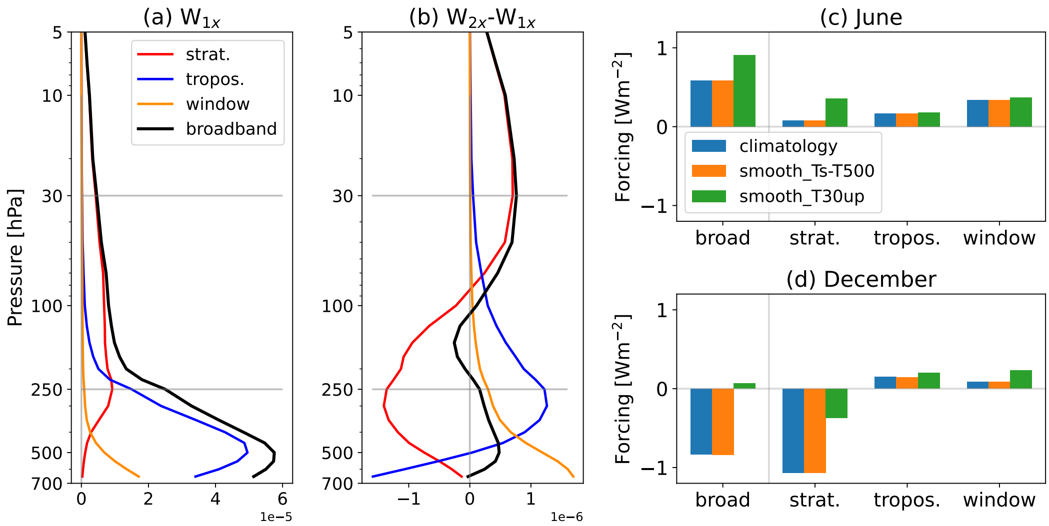

Figure 3. (a) The grouped weighting function $W(z)$ [equation (6)] of annual-mean Antarctic climate with control CO_2 for absorption lines with emission layer in the stratosphere (red), troposphere (blue), and window (yellow). The broadband $W(z)$ (sum of all groups) is shown in black. (b) Same as (a) but for the change of $W(z)$ from CO_2 doubling. (c)-(d) The TOA forcing of temperature modification experiments for Antarctica sounding in June and December. See section 3.1 for experiment design.

Figure 3a presents the grouped $W(z)$ according to (6). In general, $W(z)$ in the stratosphere, troposphere, and window groups have a maximum of $W(z)$ in the associated pressure level, respectively. The broadband $W(z)$ has a peak at around 500hPa, meaning that in Antarctica, most of the upwelling longwave at the TOA comes from around the lower troposphere with associated emission temperature. The change of $W(z)$ by CO_2 doubling is shown in Figure 3b. At first glance, an upward shift of the emission layer is clear in the stratosphere and troposphere groups: $\Delta W(z)$ of the stratosphere group is positive above 100 hPa and negative below, and $\Delta W(z)$ of the troposphere group is positive in the upper troposphere and negative in the lower troposphere. $\Delta W(z)$ of the window group is positive with a bottom-heavy structure, which implies increasing emissions from all levels with the largest increase in near-surface. This is because $\tau_g(z_{sfc})$ is smaller than unity in the window group so that the conventional definition of the emission layer $\tau_g(z_{sfc}) = 1$ lies below the surface. Overall, there is a strong cancellation below 100hPa across all groups, and the major broadband $\Delta W(z)$ is in the stratosphere.

Figures 3c–d show the decomposed forcing change of temperature modification experiments (section 3.1) in weighting function groups to evaluate the forcing sensitivity to the temperature structure. We only show the decomposed forcing of Antarctic summer (December) and winter (June), as the results in other seasons are qualitatively similar. Comparing the climatology and smooth_Ts-T500, the near-surface inversion has almost no effect: not only for the broadband forcing, but also for the troposphere and window groups. This is because there is also a surface contribution due to non-zero $W(z)$ there, and the additional CO_2 increases ϵ_{ATM} [the integral of $W(z)$ with respect to height]. This term not only slightly increases the atmosphere's emission-to-space but also blocks emission from the surface by decreasing $Tr(0)$. Both contributions combined are small.

In contrast, smooth_T30up has an anomalous positive forcing in the stratosphere group. This is consistent with an upward shift of $W(z)$ into the modified colder stratosphere (less negative lapse rate) reducing emission to space, which makes the forcing less negative or positive. This also supports the argument that the emission temperature change owing to stratospheric temperature structure is key to a negative forcing. Aside from the stratosphere group, smooth_T30up increases the forcing from the troposphere and the window groups because $2{\times}CO_2$ also increases their $\Delta W(z)$ in the stratosphere, though the change is an order smaller than in the near-surface.

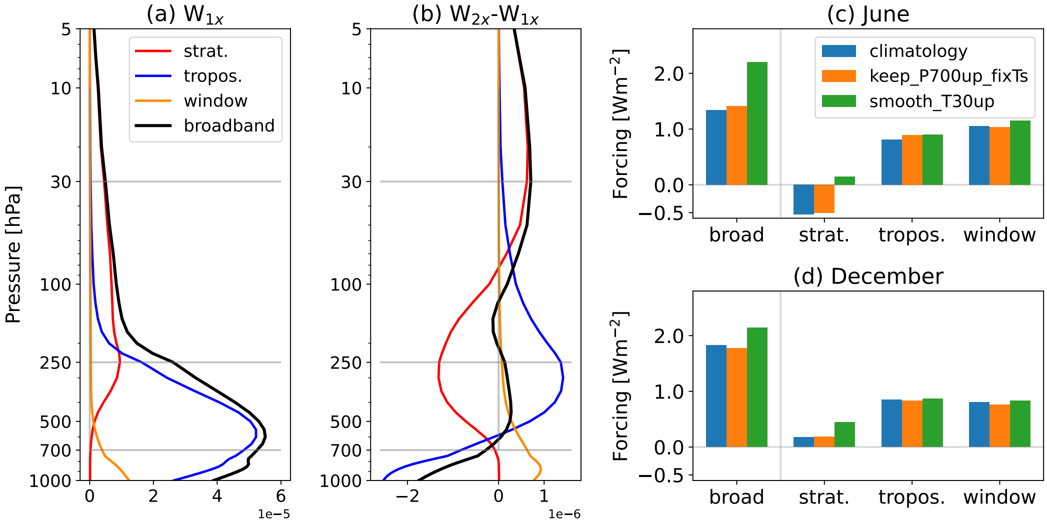

Figure 4. Same as Figure 3 but for the Arctic. See section 3.3 for experiment design.

3.3 Forcing asymmetry between the Arctic and Antarctica

While the Arctic can have, at times, negative CO_2 forcing (Fig. 1a), what accounts for the mean difference between polar regions? The Arctic forcing is overall $1-2\,\mathrm{Wm}^{-2}$ larger than Antarctica and is always positive for climatological conditions (Fig. 2c). Figures 4a,b show that $\Delta W(z)$ above 700 hPa in the Arctic is similar to Antarctica, with a large broadband $\Delta W(z)$ in the stratosphere. A contrast here is that the broadband $\Delta W(z)$ turns negative below 700 hPa. We extend the temperature modification experiments to the Arctic. In addition to smooth_T30up, we quantify how the bottom 300 hPa air mass affects the forcing by truncating the sounding at 700 hPa (keep_P700up_fixTs), with T_{SFC} unchanged. Similar to Antarctica, smooth_T30up enhances forcing in all seasons, whereas keep_P700up_fixTs does not show obvious differences (Fig. 2c).

The decomposed forcing in Figures 4c,d shows that the stratosphere group has weakly positive or negative forcing with the climatological profile. Smooth_T30up, which cools the stratosphere, increases the forcing by $0.3-0.8$ Wm^{-2}. Surprisingly, keep_P700up_fixTs removes the negative $\Delta W(z)$ in the lower troposphere but barely changes the forcing. This results from the base state difference: a thinner atmosphere is more transparent, and Tr is more sensitive to CO_2 changes. Even though keep_P700up_fixTs seemly excludes the positive forcing stemming from negative $\Delta W(z)$ in the bottom 300 hPa, a larger decrease in $Tr(0)$ increases the forcing and the net effect is small. As the forcing from

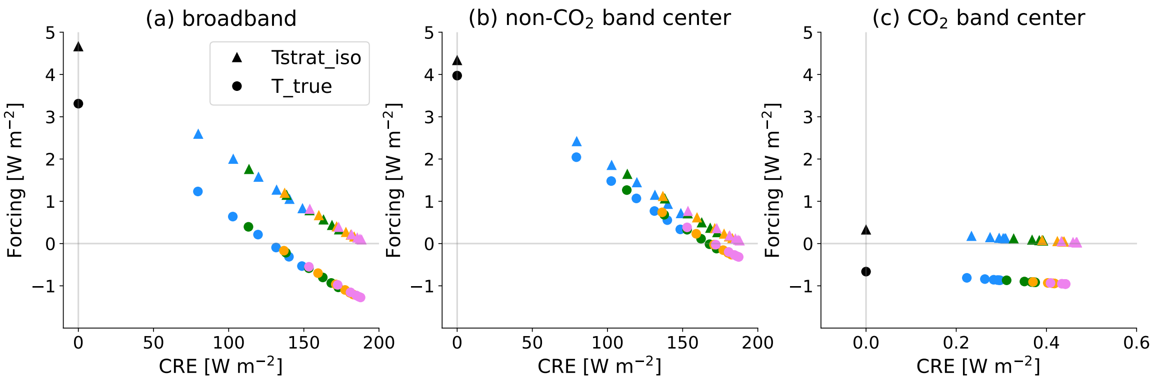

Figure 5. All-sky forcing with a tropical-mean sounding (circles) and tropical-mean sounding but with isothermal stratosphere with cold point temperature above 100 hPa (triangles) for (a) broadband forcing, (b) non-CO_2 absorption band center (bands other than 630-700 cm^{-1}), and (c) CO_2 absorption band center (630-700 cm^{-1}). Color marks the cloud ice mixing ratio from less to more with blue to red. The horizontal axis is the CRE of the specified band. The black marker where the CRE equals zero is the clear-sky forcing.

the troposphere and window groups are both larger than Antarctica by about 0.5−1 Wm^{-2}, a negative forcing in the Arctic requires an extraordinarily warm stratosphere like in a sudden stratospheric warming (Fig. 1a).

While our results consistently indicate an important role of stratospheric temperature inversion for TOA forcing, a different approach to changing the near-surface inversion and truncating the sounding might affect the interpretation. For example, Flanner et al. (2018) removed the inversion by increasing low-level temperature and T_{SFC} by up to 30 K and showed that the negative forcing vanishes. Yet, T_{SFC} increase essentially increases the surface contribution of the TOA forcing [first term of RHS in (1)]. This implicitly suggested negative forcing would be rare in the Arctic, as T_{SFC} there is ≈ 30 K warmer than Antarctica. Likewise, if a lower T_{SFC} is used for Arctic truncation experiments, the forcing will be considerably smaller but still positive (not shown).

4 Negative CO_2 forcing under all-sky conditions

Clouds are known to reduce the CO_2 forcing (Govindasamy & Caldeira, 2000). Here, we examine the role of clouds in reducing tropical forcing (Fig. 1) and assess the role of stratosphere temperature structure in reducing the forcing, as was important for the clear-sky forcing in Antarctica.

We compute forcing with different clouds using a tropical-mean sounding. For simplicity, we employ single-layer slab clouds with 100% cloud fraction and the cloud ice mixing ratio ranges linearly from 1.5×10^{-5} to 4.5×10^{-5}. The cloud tops are fixed at the tropopause (100 hPa), with the cloud bottoms varying between 125–250 hPa. These parameters create a range of longwave CRE from 50 $\mathrm{Wm^{-2}}$ to 190 $\mathrm{Wm^{-2}}$. To assess the role of the stratosphere, the all-sky forcing is computed with a similar sounding but with an isothermal stratosphere, where the stratospheric temperatures are fixed at the cold point temperature (100 hPa here), a common simplification in analytical radiative forcing/feedback analyses (Jeevanjee & Fueglistaler, 2020; Romps et al., 2022; Koll et al., 2023).

Figure 5a shows a linear dependence of broadband all-sky forcing on CRE. This is consistent with the Chen et al. (2023) for the $2\times CO_2$ forcing reduction by clouds with a linear regression model with longwave CRE as the predictor:

$$\Delta F_{cld} = -0.57 - 0.53\frac{\mathrm{CRE} - 20.06}{20.06}, \tag{7}$$

where ΔF_{cld} is the forcing difference under all-sky and clear-sky conditions. Interestingly, the forcing changes sign at 120 $\mathrm{Wm^{-2}}$, which can be predicted by the regression model as the CRE required to zero 3.2 $\mathrm{Wm^{-2}}$ clear-sky forcing. An isothermal stratosphere barely changes CRE, and the forcing approaches but never goes below zero.

Since clouds feature strong, spectrally-broad absorption, the refined $g-$point-based decomposition (section 3.2) is gratuitous. We instead use RRTMG's built-in output bands for all-sky analyses. In the tropics, the stratosphere's role in forcing largely arises from the CO_2 absorption band center (630-700 $\mathrm{cm^{-1}}$). This band dominates the forcing difference between the control and isothermal stratosphere (Figs. 5b,c). Figure 5b further shows that the clouds impose strong masking effects in the non-CO_2 band, consistent with expectations that clouds reduce forcing everywhere other than the stratosphere component. The negative forcing mainly comes from CO_2 band center (Fig. 5c), where the emission is dominated by the stratosphere, and forcing remains positive with an isothermal stratosphere. We conclude that the negative forcing under all-sky results from increased emission from the stratosphere in response to CO_2. As the positive forcing from the troposphere and the window are usually large in the tropics, negative forcing from the stratosphere wins only when the contribution below tropopause is reduced by clouds with strong CRE.

5 Conclusion

This study explores the CO_2 forcing sensitivity to the vertical temperature structure, with an emphasis on what leads to a small, and even negative TOA forcing in the current climate. Two climate states with negative CO_2 forcing are discussed: the polar regions and the tropics. In brief, a negative forcing demands strong negative forcing from the stratosphere (enhanced emission-to-space mainly from CO_2 absorption band center near 660 cm^{-1}) and relatively weak forcing from the combined contribution from the troposphere and window (mainly from other parts of spectra with where CO_2 is less absorbing). These two components depend on the stratospheric and near-surface temperature, respectively. In polar climates, the effect of near-surface temperature structure is muted because the emission layer changes within the troposphere and the surface contribution counteract each other. The forcing is thus insensitive to the tropospheric temperature structure, at odds with the conventional argument that the near-surface inversion is key to negative forcing in Antarctica (Flanner et al., 2018; Sejas et al., 2018). In the tropics, there is abundant forcing coming from the troposphere and the window (i.e., away from the CO_2 absorption center). Therefore, a strong CRE is essential to mask the forcing stemming from the troposphere to enable the strong emission-to-space from the stratosphere to turn the broadband forcing negative.

Two major factors that make the current Antarctic climate a distinct region with negative CO_2 forcing include the low surface temperature, which reduces positive forcing, and the high stratospheric temperature, which enhances negative forcing. Both factors are less extreme in the Arctic climate. There are still rare occasions when there is negative CO_2 forcing in the Arctic, such as during the strong sudden stratospheric warming events when the stratosphere warms by tens of K (e.g., Baldwin et al., 2021).

By examining the cause of negative CO_2 forcing, this study highlights the stratosphere's role in shaping the TOA forcing. It also demonstrates the value of resolving the spectral dimension of radiation. Simple gray-radiation, broadband optical depth perspectives (e.g., equation 5) that do not identify spectral emission characteristics would lead to inaccurate radiation sensitivity to either surface or stratospheric temperature. Other greenhouse gases (e.g., CH_4) with less strong absorption band centers may behave differently because of smaller $\Delta W(z)$ in the stratosphere, an interesting area for future research.

Our analysis here focuses on the spectral competition that can give rise to negative TOA forcing, though this competition is also relevant to small-but-positive forcing. We also reiterate that negative TOA forcing does not imply that additional CO_2 cools the surface, as adjustments are important to the re-establishment of Antarctica energy balance (Smith et al., 2018). The interplay between the vertical forcing variation of a particular forcing agent and the accompanying temperature adjustments warrants further investigation.

6 Open Research

The ERA5 dataset can be accessed through the ECMWF website (https://cds.climate.copernicus.eu/). The RRTMG is available at http://rtweb.aer.com/rrtm_frame.html. The scripts to generate data and figures are available at https://doi.org/10.5281/zenodo.8358357.

Acknowledgments

We acknowledge the supports of the Natural Sciences and Engineering Research Council of Canada (RGPIN-2019-04511) and Fonds de Recherche Nature et Technologies of Quebec (2021-PR-283823). YTC acknowledges the supports of Stephen & Anastasia Mysak Fellowship of McGill University.

References

Baldwin, M. P., Ayarzagüena, B., Birner, T., Butchart, N., Butler, A. H., Charlton-Perez, A. J., ... Pedatella, N. M. (2021). Sudden stratospheric warmings. *Reviews of Geophysics*, *59*(1), e2020RG000708. (e2020RG000708 10.1029/2020RG000708) doi: https://doi.org/10.1029/2020RG000708

Chen, Y.-T., Huang, Y., & Merlis, T. M. (2023). The global patterns of instantaneous CO_2 forcing at the top of the atmosphere and the surface. *Journal of Climate*, *36*(18), 6331 - 6347. doi: https://doi.org/10.1175/JCLI-D-22-0708.1

Flanner, M. G., Huang, X., Chen, X., & Krinner, G. (2018). Climate response to negative greenhouse gas radiative forcing in polar winter. *Geophys. Res. Lett.*, *45*(4), 1997–2004.

Freese, L. M., & Cronin, T. W. (2021). Antarctic radiative and temperature responses to a doubling of CO_2. *Geophys. Res. Lett.*, *48*(17), e2021GL093676.

Fu, Q., & Liou, K. N. (1992). On the correlated k-distribution method for radiative transfer in nonhomogeneous atmospheres. *Journal of Atmospheric Sciences*, *49*(22), 2139 - 2156.

Govindasamy, B., & Caldeira, K. (2000). Geoengineering Earth's radiation balance to mitigate CO_2-induced climate change. *Geophys. Res. Lett.*, *27*, 2141–2144.

Hersbach, H., Bell, B., Berrisford, P., Hirahara, S., Horányi, A., Muñoz-Sabater, J., ... Thépaut, J.-N. (2020). The ERA5 global reanalysis. *Quarterly Journal of the Royal Meteorological Society*, *146*(730), 1999-2049. doi: https://doi.org/10.1002/qj.3803

Huang, Y., & Bani Shahabadi, M. (2014). Why logarithmic? A note on the dependence of radiative forcing on gas concentration. *J. Geophys. Res. Atmospheres*, *119*(24), 13,683-13,689.

Huang, Y., Tan, X., & Xia, Y. (2016). Inhomogeneous radiative forcing of homogeneous greenhouse gases. *J. Geophys. Res.*, *121*, 2780–2789.

Jeevanjee, N., & Fueglistaler, S. (2020). On the cooling-to-space approximation. *J. Atmos. Sci.*, *77*(2), 465 - 478. doi: 10.1175/JAS-D-18-0352.1

Jeevanjee, N., Seeley, J., Paynter, D., & Fueglistaler, S. (2021). An analytical model for spatially varying clear-sky CO_2 forcing. *Journal of Climate*, *34*(23), 9463 - 9480.

Koll, D. D. B., Jeevanjee, N., & Lutsko, N. J. (2023). An analytic model for the clear-sky longwave feedback. *Journal of the Atmospheric Sciences*, *80*(8), 1923 - 1951. doi: https://doi.org/10.1175/JAS-D-22-0178.1

Mlawer, E. J., Taubman, S. J., Brown, P. D., Iacono, M. J., & Clough, S. A. (1997). Radiative transfer for inhomogeneous atmospheres: RRTM, a validated correlated-k model for the longwave. *Journal of Geophysical Research: Atmospheres*, *102*(D14), 16663-16682. doi: https://doi.org/10.1029/97JD00237

Romps, D. M., Seeley, J. T., & Edman, J. P. (2022). Why the forcing from carbon dioxide scales as the logarithm of its concentration. *J. of Climate*, *35*(13), 4027–4047.

Schmithüsen, H., Notholt, J., König-Langlo, G., Lemke, P., & Jung, T. (2015). How increasing CO_2 leads to an increased negative greenhouse effect in Antarctica.

Geophys. Res. Lett., *42*(23), 10,422–10,428.

Sejas, S. A., aylor, P. C., & Cai, M. (2018). Unmasking the negative greenhouse effect over the Antarctic Plateau. *npj Climate and Atmospheric Science*, *1*(17), 2397–3722.

Smith, K. L., Chiodo, G., Previdi, M., & Polvani, L. M. (2018). No surface cooling over antarctica from the negative greenhouse effect associated with instantaneous quadrupling of CO_2 concentrations. *Journal of Climate*, *31*(1), 317 - 323. doi: https://doi.org/10.1175/JCLI-D-17-0418.1

Zhang, M., & Huang, Y. (2014). Radiative forcing of quadrupling CO_2. *J. Climate*, *27*, 2496–2508.

The cause of negative CO_2 forcing at the top-of-atmosphere: the role of stratospheric vs. tropospheric temperature inversions

Yan-Ting Chen[1], Timothy M. Merlis[2], and Yi Huang[1]

[1]Department of Atmospheric and Oceanic Sciences, McGill University, Montreal, Quebec, Canada
[2]Program in Atmospheric and Oceanic Sciences, Princeton University, Princeton, NJ, USA

Key Points:

- In addition to Antarctica, increased CO_2 increases OLR in the Arctic and deep tropics under certain circumstances.
- In polar regions, negative CO_2 forcing arises from stratospheric temperature inversions, while near-surface inversions have a small effect.
- CO_2 forcing can be negative in other regions when the high clouds block the tropospheric emission, leaving the stratospheric contribution.

Corresponding author: Yan-Ting Chen, `yan-ting.chen@mail.mcgill.ca`

Abstract

Increasing carbon dioxide (CO_2) in the atmosphere usually reduces Earth's outgoing longwave radiation (OLR). The unusual case of Antarctica, where CO_2 enhances OLR and implies a negative forcing, has previously been explained by the strong near-surface inversion or extremely low surface temperature. However, negative forcing can occasionally be found in the Arctic and tropics where neither of these explanations applies. Here, we examine the changes in infrared opacity from CO_2 doubling in these low or negative forcing climate states, which shows the predominant role of the stratospheric contribution to the broadband forcing. Negative forcing in today's climate demands a combination of strong negative forcing caused by a steep stratospheric temperature inversion and a weaker positive forcing in the atmospheric window, which can be caused by a low surface temperature or a strong high cloud masking effect. Contrary to conventional wisdom, the near-surface inversion has little impact on the forcing.

Plain Language Summary

CO_2, as an important greenhouse gas, is known to reduce the Earth's longwave emission, provoking a positive forcing that increases the net flow of energy into the Earth system. In this study, we discuss the cause of negative forcing, where CO_2 increases longwave emission that happens most commonly in Antarctica and in some rare conditions in the Arctic and tropics. In contrast to conventional arguments that a near-surface temperature increase with altitude is key to a negative forcing, we show that the stratospheric temperature and, in the tropics, clouds play a more important role. The results are based on temperature modification experiments and an analysis of the vertical structure of atmospheric emission changes. While a negative forcing does not mean the surface would cool since there are other important adjustments involved in the re-establishment of energy balance, the results show the values of resolving the spectral dimension of radiation to quantify the radiative sensitivity to the near-surface and stratosphere temperature structure.

1 Introduction

It is known that increasing carbon dioxide (CO_2) concentration enhances the greenhouse effect and results in positive longwave radiative forcing at the top-of-atmosphere (TOA), leading to an increase in Earth's radiation budget. While this is true in general, it has also been shown that the CO_2 forcing can enhance longwave emission-to-space in Antarctica, which is a negative TOA forcing. Such phenomenon is found in radiative transfer calculations (Zhang & Huang, 2014; Flanner et al., 2018; Jeevanjee et al., 2021; Freese & Cronin, 2021; Chen et al., 2023) and climate models (Schmithüsen et al., 2015; Huang et al., 2016; Smith et al., 2018), with support from observations (Schmithüsen et al., 2015; Sejas et al., 2018). Although a negative TOA forcing there might not translate to surface cooling (Smith et al., 2018; Freese & Cronin, 2021), understanding what distinguishes the radiative forcing in Antarctica from other parts of the climate helps improve theoretical understanding of the radiative forcing.

Existing understandings from spectral radiative transfer properties sheds light on negative TOA forcing from increased CO_2. This can result from the non-monotonic vertical temperature structure. In a non-scattering atmosphere, the radiative fluxes at the TOA ($z = \infty$) at a wavenumber ν can be written as:

$$I_\nu(\infty) = B_\nu(0)\, Tr_\nu(0) + \int_0^\infty B_\nu(z)\, W_\nu(z)\, dz, \tag{1}$$

$$Tr_\nu(z) \equiv e^{-\tau_\nu(z)}, \tag{2}$$

$$W_\nu(z) \equiv \frac{dTr_\nu(z)}{dz}, \tag{3}$$

where I_ν is the monochromatic radiance, $B_\nu(z)$ is the thermal emission of the layer at the height z, $Tr_\nu(z)$ is the transmissivity between z and the TOA. $\tau_\nu(z)$ is the optical depth between the TOA and z that monotonically increases from the TOA to the surface, and $W_\nu(z)$, the weighting function, is the derivative of the transmission function with height.

As CO_2 increases, the altitude of the weighting function peak, or the so-called emission layer where $\tau_\nu(z) = 1$, shifts to a higher level (e.g., Huang & Bani Shahabadi, 2014). When collocated with a temperature inversion, the elevated emission layer enhances emission-to-space from the warmer air (as opposed to having colder air above, as is typical in the troposphere) and therefore leads to a negative TOA forcing. Such negative forcing in monochromatic radiance has been identified in individual wavelengths where the emission layer shifts within either stratospheric (Huang & Bani Shahabadi, 2014) or near-surface (Flanner et al., 2018; Sejas et al., 2018) temperature inversion. As the gas absorption properties vary spectrally, the behavior at a single wavelength does not determine the broadband results. Antarctica, interestingly, is a region where the negative forcing remains after spectral integration.

From a simplified, broadband perspective, Schmithüsen et al. (2015) and Smith et al. (2018) approximated the TOA forcing with a two-level model. Assuming an effective emission temperature of the atmosphere and the Earth's surface is a blackbody, the outgoing longwave radiation (OLR) at the TOA is expressed as:

$$\mathrm{OLR} = (1-\epsilon_{ATM})\sigma T_{SFC}^4 + \epsilon_{ATM}\sigma T_{ATM}^4, \tag{4}$$

where ϵ_{ATM} is the broadband emissivity of the atmosphere and equals broadband $1-Tr(0)$ in (1). As higher CO_2 concentration increases ϵ_{ATM}, the dependency of instantaneous forcing is then:

$$\frac{\partial \mathrm{OLR}}{\partial \epsilon_{ATM}} = \sigma(T_{ATM}^4 - T_{SFC}^4). \tag{5}$$

From this equation, the sign of the forcing is determined by the temperature contrast between the surface and the atmosphere: when $T_{ATM} > T_{SFC}$, OLR increases as CO_2 increases ϵ_{ATM}. Negative forcing in Antarctica is then explained by the fact that T_{SFC} in Antarctica is lower than the lower troposphere (owing to near-surface inversion) or the stratosphere. This explanation partly echoes the emission layer-based argument that the air temperature structure is important for the forcing, but T_{ATM} in (5) is not clearly defined and itself could be a function of CO_2 concentration. Moreover, the forcing caused by ϵ_{ATM} change is found positive even in Antarctica [blue dots in Figs. 9f,h of Chen et al. (2023)]. The utility of the broadband analytical model and the role of near-surface versus the stratospheric temperature structure, therefore, remains obscure.

Negative TOA forcing also happens outside of Antarctica. The Arctic sometimes exhibits strong negative forcing (Fig. 1a). Negative forcing even occurs in the tropics and mid-latitudes for instances of strong longwave cloud radiative effects (CRE), when the all-sky OLR is much lower than the clear-sky OLR. Although such extreme events are smoothed out in the long-term average, these occasions of negative forcing are worth documenting and suggest that there are other factors that can sharply modify the forcing, in addition to simple surface temperature-based or stratospheric temperature-based arguments.

This study explores the causes of negative TOA CO_2 forcing in the polar regions and tropics. The distinct climates there will generalize the current understanding of how the temperature structure and clouds shape the instantaneous CO_2 forcing at the TOA. The radiative transfer model and the dataset used here are described in Section 2. In section 3, we focus on the causes of negative forcing under clear-sky conditions, which

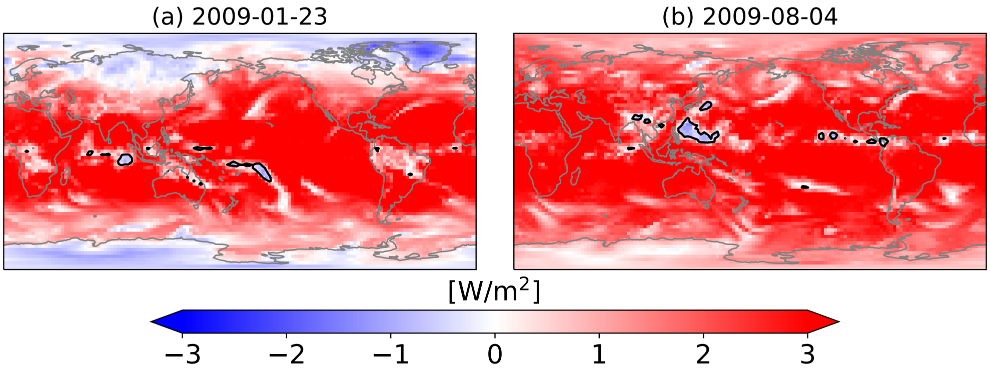

Figure 1. The daily-mean forcing pattern on (a) Jan 23, 2009, near the onset of a major mid-winter SSW event and (b) Aug 4, 2009, when there are strong cloud masking effects in the western North Pacific from intensifying typhoon Morakot. The black contour shows longwave cloud radiative effect (CRE) of 120 $\mathrm{W m^{-2}}$.

mainly occurs in Antarctica. We quantify the forcing contributed by the near-surface temperature inversion and stratospheric inversion, with a novel approach that decomposes the forcing into bulk spectral regions, which feature different sensitivities to temperature structures. We also discuss why the negative CO_2 forcing is less common in the Arctic than Antarctica. Section 4 discusses negative forcing under all-sky conditions. We also use idealized experiments, in which the temperature and clouds are modified to show how the temperature structure and clouds affect the sign of CO_2 forcing. We conclude in section 5.

2 Radiative transfer calculation

We use standalone longwave Rapid Radiative Transfer Model (RRTMG, Mlawer et al., 1997), which calculates fluxes ranging from 10 $\mathrm{cm^{-1}}$ to 3250 $\mathrm{cm^{-1}}$. The climatology of atmospheric profiles, including temperature, specific humidity, and ozone, are from ERA5 reanalysis dataset of the European Centre for Medium-Range Weather Forecasts (Hersbach et al., 2020). The radiative forcing of doubled CO_2 is calculated as the flux difference between 760 and 380 ppmv CO_2 concentrations. The concentration of other well-mixed greenhouse gases, CH_4 and N_2O, are prescribed to 1.797 and 0.323 ppmv, respectively. CFCs are not included.

RRTMG performs the radiative transfer calculation at a total of 140 g-points, with each accounting for one monochromatic spectral node where the wavenumbers with similar absorption coefficients are grouped together beforehand. The fluxes at individual g-points are summed to get the bandwise and the broadband fluxes. This technique, named the correlated-k method (Fu & Liou, 1992), is a numerical treatment that speeds up computation (vs. calculating fluxes at a small, fixed wavenumber increment like line-by-line radiative transfer).

3 Negative CO_2 forcing under clear-sky conditions

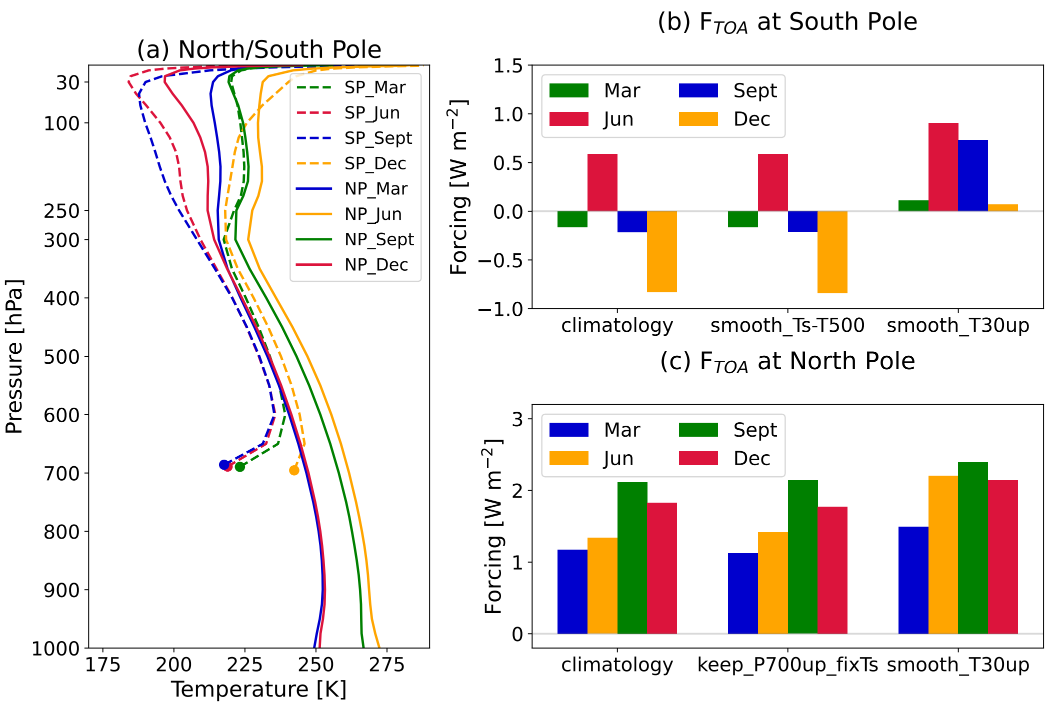

Figure 2. (a) The seasonality of climatological temperature at the South and North Pole. (b) The broadband, instantaneous CO_2 forcing at the TOA based on the climatological profile and temperature modification experiments of the South Pole (section 3.1). (c) Same as (b) but for the North Pole (section 3.3). Note that the range of y-axis in (b) and (c) is different.

3.1 Temperature modification experiments

To evaluate the role of inversions on CO_2 forcing, we calculate the forcing with modified temperature soundings of the South Pole. Specifically, the near-surface inversion is removed by replacing the temperature below 500 hPa with temperature at the 500 hPa (smooth_Ts-T500), and the stratospheric inversion is removed by setting temperature above 30 hPa with temperature at the 30 hPa (smooth_T30up). In both experiments, we choose to leave T_{SFC} unperturbed because T_{SFC} determines the upward longwave emission, which is an important energetic constraint. How T_{SFC} itself affects the forcing will be discussed at the end of this section. The water vapor in the polar regions is scarce and does not change the results qualitatively, so we keep using climatological water vapor profiles to highlight the role of temperature structure even if the near-surface layer might be supersaturated when the near-surface temperature is reduced.

Figures 2a,b plot the climatological temperature profile at the South Pole and the resulting instantaneous CO_2 forcing. Consistent with previous literature, the CO_2 forcing is found negative throughout September to March (Schmithüsen et al., 2015; Smith et al., 2018; Freese & Cronin, 2021; Chen et al., 2023). We note that December features the strongest negative forcing yet the near-surface inversion is the weakest. Surprisingly, despite large temperature reductions imposed in smooth_Ts-T500 experiment sometimes exceeds 20 K in the lower troposphere, the forcing changes by less than $0.01\,\mathrm{Wm}^{-2}$. In contrast, the changes in the stratospheric lapse rate in smooth_T30up effectively eliminate the negative forcing and can increase the forcing by $\sim 1\,\mathrm{Wm}^{-2}$. These suggest a dominant role of stratospheric temperature in modifying the CO_2 forcing, at least when T_{SFC} remains unchanged.

3.2 Attributing the radiative forcing to the temperature profile

According to (1), the flux at the TOA comes from various altitudes of the atmosphere owing to the wavelength-varying $\tau_\nu(z)$ and $W_\nu(z)$ structure. In other words, one can relate the forcing and the contributing atmospheric level by calculating $W_\nu(z)$ in (3) once $\tau_\nu(z)$ is known.

We exploit the spectral information in the model by outputting the optical depth and radiative fluxes at all 140 g-points, and regroup the g-point-based fluxes according to which part of the atmosphere the climatological emission layer $[\tau_g(z) = 1]$ belongs to. The g-point-based fluxes are sorted into three groups with the following definitions:

- Stratosphere: g-points which $\tau_g(z_{250}) > 1$.
- Troposphere: g-points which $\tau_g(z_{250}) < 1$ and $\tau_g(z_{sfc}) > 1$.

- Window: g-points which $\tau_g(z_{sfc}) < 1$.

The subscript of z denotes the associated pressure level, and the tropopause is set at 250 hPa for convenience. In this definition, the first term on the RHS of (1), the forcing coming from the surface, is included in the window group. Together with (3), the g-point grouped weighting function is calculated as:

$$W_i(z) = \frac{1}{I(0)} \sum_{g=0}^{n} I_g(0) \cdot \frac{dTr_g(z)}{dz}, \tag{6}$$

where the subscript g denotes the fluxes in the g-point dimension and the sum is over the g-points where the emission layer lies in the atmospheric layer group i defined above. Compared to using RRTMG's 16-band outputs that are segregated by respective gas absorption properties beforehand, this method offers a finer view of what part of the atmospheric profile contributes to the radiative fluxes.

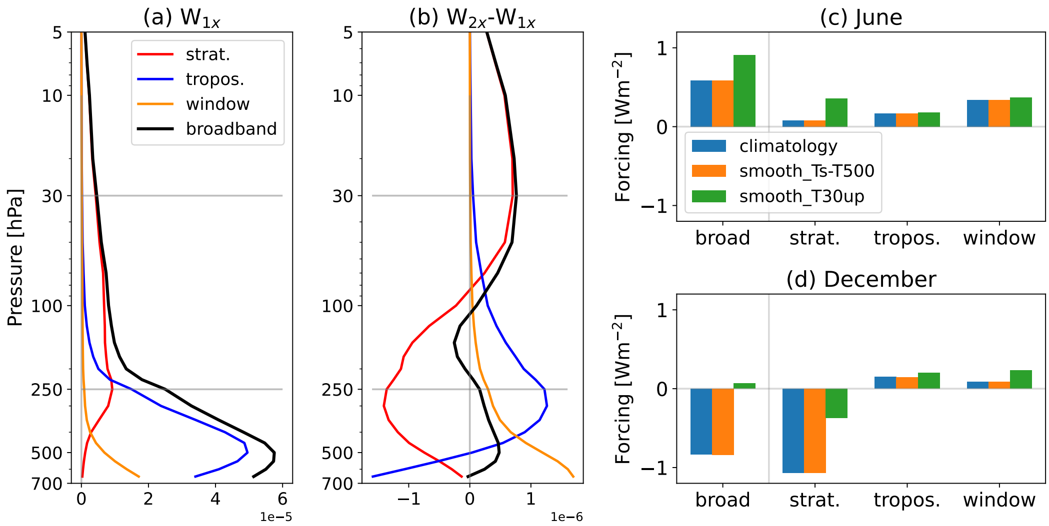

Figure 3. (a) The grouped weighting function $W(z)$ [equation (6)] of annual-mean Antarctic climate with control CO_2 for absorption lines with emission layer in the stratosphere (red), troposphere (blue), and window (yellow). The broadband $W(z)$ (sum of all groups) is shown in black. (b) Same as (a) but for the change of $W(z)$ from CO_2 doubling. (c)-(d) The TOA forcing of temperature modification experiments for Antarctica sounding in June and December. See section 3.1 for experiment design.

Figure 3a presents the grouped $W(z)$ according to (6). In general, $W(z)$ in the stratosphere, troposphere, and window groups have a maximum of $W(z)$ in the associated pressure level, respectively. The broadband $W(z)$ has a peak at around 500hPa, meaning that in Antarctica, most of the upwelling longwave at the TOA comes from around the lower troposphere with associated emission temperature. The change of $W(z)$ by CO_2 doubling is shown in Figure 3b. At first glance, an upward shift of the emission layer is clear in the stratosphere and troposphere groups: $\Delta W(z)$ of the stratosphere group is positive above 100 hPa and negative below, and $\Delta W(z)$ of the troposphere group is positive in the upper troposphere and negative in the lower troposphere. $\Delta W(z)$ of the window group is positive with a bottom-heavy structure, which implies increasing emissions from all levels with the largest increase in near-surface. This is because $\tau_g(z_{sfc})$ is smaller than unity in the window group so that the conventional definition of the emission layer $\tau_g(z_{sfc}) = 1$ lies below the surface. Overall, there is a strong cancellation below 100hPa across all groups, and the major broadband $\Delta W(z)$ is in the stratosphere.

Figures 3c–d show the decomposed forcing change of temperature modification experiments (section 3.1) in weighting function groups to evaluate the forcing sensitivity to the temperature structure. We only show the decomposed forcing of Antarctic summer (December) and winter (June), as the results in other seasons are qualitatively similar. Comparing the climatology and smooth_Ts-T500, the near-surface inversion has almost no effect: not only for the broadband forcing, but also for the troposphere and window groups. This is because there is also a surface contribution due to non-zero $W(z)$ there, and the additional CO_2 increases ϵ_{ATM} [the integral of $W(z)$ with respect to height]. This term not only slightly increases the atmosphere's emission-to-space but also blocks emission from the surface by decreasing $Tr(0)$. Both contributions combined are small.

In contrast, smooth_T30up has an anomalous positive forcing in the stratosphere group. This is consistent with an upward shift of $W(z)$ into the modified colder stratosphere (less negative lapse rate) reducing emission to space, which makes the forcing less negative or positive. This also supports the argument that the emission temperature change owing to stratospheric temperature structure is key to a negative forcing. Aside from the stratosphere group, smooth_T30up increases the forcing from the troposphere and the window groups because $2\times CO_2$ also increases their $\Delta W(z)$ in the stratosphere, though the change is an order smaller than in the near-surface.

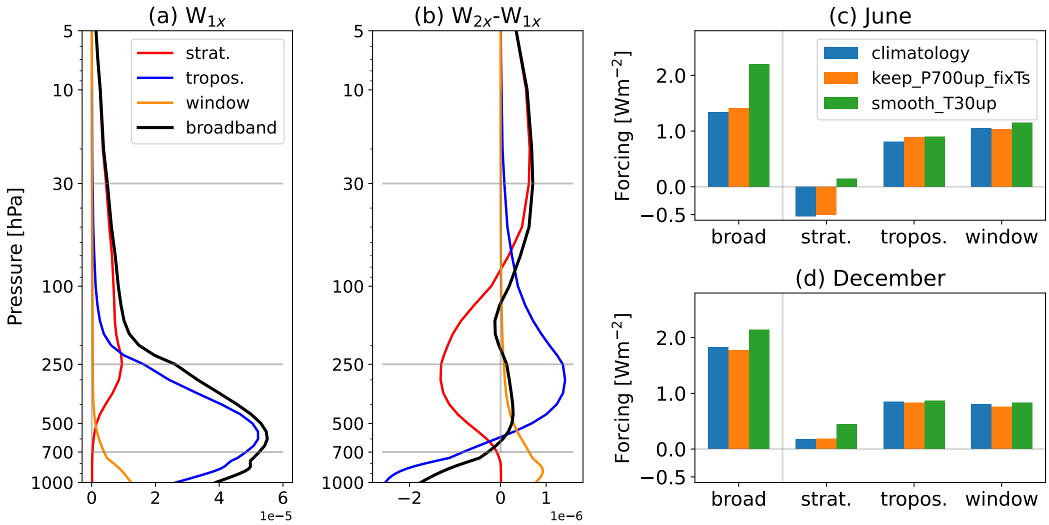

Figure 4. Same as Figure 3 but for the Arctic. See section 3.3 for experiment design.

3.3 Forcing asymmetry between the Arctic and Antarctica

While the Arctic can have, at times, negative CO_2 forcing (Fig. 1a), what accounts for the mean difference between polar regions? The Arctic forcing is overall $1-2\,\mathrm{Wm}^{-2}$ larger than Antarctica and is always positive for climatological conditions (Fig. 2c). Figures 4a,b show that $\Delta W(z)$ above 700 hPa in the Arctic is similar to Antarctica, with a large broadband $\Delta W(z)$ in the stratosphere. A contrast here is that the broadband $\Delta W(z)$ turns negative below 700 hPa. We extend the temperature modification experiments to the Arctic. In addition to smooth_T30up, we quantify how the bottom 300 hPa air mass affects the forcing by truncating the sounding at 700 hPa (keep_P700up_fixTs), with T_{SFC} unchanged. Similar to Antarctica, smooth_T30up enhances forcing in all seasons, whereas keep_P700up_fixTs does not show obvious differences (Fig. 2c).

The decomposed forcing in Figures 4c,d shows that the stratosphere group has weakly positive or negative forcing with the climatological profile. Smooth_T30up, which cools the stratosphere, increases the forcing by $0.3-0.8$ Wm^{-2}. Surprisingly, keep_P700up_fixTs removes the negative $\Delta W(z)$ in the lower troposphere but barely changes the forcing. This results from the base state difference: a thinner atmosphere is more transparent, and Tr is more sensitive to CO_2 changes. Even though keep_P700up_fixTs seemly excludes the positive forcing stemming from negative $\Delta W(z)$ in the bottom 300 hPa, a larger decrease in $Tr(0)$ increases the forcing and the net effect is small. As the forcing from

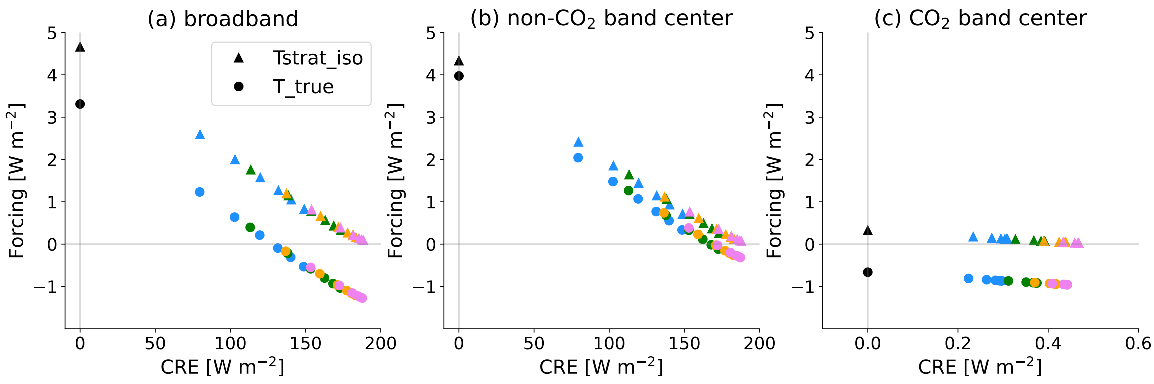

Figure 5. All-sky forcing with a tropical-mean sounding (circles) and tropical-mean sounding but with isothermal stratosphere with cold point temperature above 100 hPa (triangles) for (a) broadband forcing, (b) non-CO_2 absorption band center (bands other than 630-700 cm^{-1}), and (c) CO_2 absorption band center (630-700 cm^{-1}). Color marks the cloud ice mixing ratio from less to more with blue to red. The horizontal axis is the CRE of the specified band. The black marker where the CRE equals zero is the clear-sky forcing.

the troposphere and window groups are both larger than Antarctica by about 0.5−1 Wm^{-2}, a negative forcing in the Arctic requires an extraordinarily warm stratosphere like in a sudden stratospheric warming (Fig. 1a).

While our results consistently indicate an important role of stratospheric temperature inversion for TOA forcing, a different approach to changing the near-surface inversion and truncating the sounding might affect the interpretation. For example, Flanner et al. (2018) removed the inversion by increasing low-level temperature and T_{SFC} by up to 30 K and showed that the negative forcing vanishes. Yet, T_{SFC} increase essentially increases the surface contribution of the TOA forcing [first term of RHS in (1)]. This implicitly suggested negative forcing would be rare in the Arctic, as T_{SFC} there is ≈ 30 K warmer than Antarctica. Likewise, if a lower T_{SFC} is used for Arctic truncation experiments, the forcing will be considerably smaller but still positive (not shown).

4 Negative CO_2 forcing under all-sky conditions

Clouds are known to reduce the CO_2 forcing (Govindasamy & Caldeira, 2000). Here, we examine the role of clouds in reducing tropical forcing (Fig. 1) and assess the role of stratosphere temperature structure in reducing the forcing, as was important for the clear-sky forcing in Antarctica.

We compute forcing with different clouds using a tropical-mean sounding. For simplicity, we employ single-layer slab clouds with 100% cloud fraction and the cloud ice mixing ratio ranges linearly from 1.5×10^{-5} to 4.5×10^{-5}. The cloud tops are fixed at the tropopause (100 hPa), with the cloud bottoms varying between 125–250 hPa. These parameters create a range of longwave CRE from 50 $\mathrm{Wm^{-2}}$ to 190 $\mathrm{Wm^{-2}}$. To assess the role of the stratosphere, the all-sky forcing is computed with a similar sounding but with an isothermal stratosphere, where the stratospheric temperatures are fixed at the cold point temperature (100 hPa here), a common simplification in analytical radiative forcing/feedback analyses (Jeevanjee & Fueglistaler, 2020; Romps et al., 2022; Koll et al., 2023).

Figure 5a shows a linear dependence of broadband all-sky forcing on CRE. This is consistent with the Chen et al. (2023) for the $2\times CO_2$ forcing reduction by clouds with a linear regression model with longwave CRE as the predictor:

$$\Delta F_{cld} = -0.57 - 0.53\frac{\mathrm{CRE} - 20.06}{20.06}, \tag{7}$$

where ΔF_{cld} is the forcing difference under all-sky and clear-sky conditions. Interestingly, the forcing changes sign at 120 $\mathrm{Wm^{-2}}$, which can be predicted by the regression model as the CRE required to zero 3.2 $\mathrm{Wm^{-2}}$ clear-sky forcing. An isothermal stratosphere barely changes CRE, and the forcing approaches but never goes below zero.

Since clouds feature strong, spectrally-broad absorption, the refined $g-$point-based decomposition (section 3.2) is gratuitous. We instead use RRTMG's built-in output bands for all-sky analyses. In the tropics, the stratosphere's role in forcing largely arises from the CO_2 absorption band center (630-700 $\mathrm{cm^{-1}}$). This band dominates the forcing difference between the control and isothermal stratosphere (Figs. 5b,c). Figure 5b further shows that the clouds impose strong masking effects in the non-CO_2 band, consistent with expectations that clouds reduce forcing everywhere other than the stratosphere component. The negative forcing mainly comes from CO_2 band center (Fig. 5c), where the emission is dominated by the stratosphere, and forcing remains positive with an isothermal stratosphere. We conclude that the negative forcing under all-sky results from increased emission from the stratosphere in response to CO_2. As the positive forcing from the troposphere and the window are usually large in the tropics, negative forcing from the stratosphere wins only when the contribution below tropopause is reduced by clouds with strong CRE.

5 Conclusion

This study explores the CO_2 forcing sensitivity to the vertical temperature structure, with an emphasis on what leads to a small, and even negative TOA forcing in the current climate. Two climate states with negative CO_2 forcing are discussed: the polar regions and the tropics. In brief, a negative forcing demands strong negative forcing from the stratosphere (enhanced emission-to-space mainly from CO_2 absorption band center near 660 cm^{-1}) and relatively weak forcing from the combined contribution from the troposphere and window (mainly from other parts of spectra with where CO_2 is less absorbing). These two components depend on the stratospheric and near-surface temperature, respectively. In polar climates, the effect of near-surface temperature structure is muted because the emission layer changes within the troposphere and the surface contribution counteract each other. The forcing is thus insensitive to the tropospheric temperature structure, at odds with the conventional argument that the near-surface inversion is key to negative forcing in Antarctica (Flanner et al., 2018; Sejas et al., 2018). In the tropics, there is abundant forcing coming from the troposphere and the window (i.e., away from the CO_2 absorption center). Therefore, a strong CRE is essential to mask the forcing stemming from the troposphere to enable the strong emission-to-space from the stratosphere to turn the broadband forcing negative.

Two major factors that make the current Antarctic climate a distinct region with negative CO_2 forcing include the low surface temperature, which reduces positive forcing, and the high stratospheric temperature, which enhances negative forcing. Both factors are less extreme in the Arctic climate. There are still rare occasions when there is negative CO_2 forcing in the Arctic, such as during the strong sudden stratospheric warming events when the stratosphere warms by tens of K (e.g., Baldwin et al., 2021).

By examining the cause of negative CO_2 forcing, this study highlights the stratosphere's role in shaping the TOA forcing. It also demonstrates the value of resolving the spectral dimension of radiation. Simple gray-radiation, broadband optical depth perspectives (e.g., equation 5) that do not identify spectral emission characteristics would lead to inaccurate radiation sensitivity to either surface or stratospheric temperature. Other greenhouse gases (e.g., CH_4) with less strong absorption band centers may behave differently because of smaller $\Delta W(z)$ in the stratosphere, an interesting area for future research.

Our analysis here focuses on the spectral competition that can give rise to negative TOA forcing, though this competition is also relevant to small-but-positive forcing. We also reiterate that negative TOA forcing does not imply that additional CO_2 cools the surface, as adjustments are important to the re-establishment of Antarctica energy balance (Smith et al., 2018). The interplay between the vertical forcing variation of a particular forcing agent and the accompanying temperature adjustments warrants further investigation.

6 Open Research

The ERA5 dataset can be accessed through the ECMWF website (https://cds.climate.copernicus.eu/). The RRTMG is available at http://rtweb.aer.com/rrtm_frame.html. The scripts to generate data and figures are available at https://doi.org/10.5281/zenodo.8358357.

Acknowledgments

We acknowledge the supports of the Natural Sciences and Engineering Research Council of Canada (RGPIN-2019-04511) and Fonds de Recherche Nature et Technologies of Quebec (2021-PR-283823). YTC acknowledges the supports of Stephen & Anastasia Mysak Fellowship of McGill University.

References

Baldwin, M. P., Ayarzagüena, B., Birner, T., Butchart, N., Butler, A. H., Charlton-Perez, A. J., … Pedatella, N. M. (2021). Sudden stratospheric warmings. *Reviews of Geophysics*, *59*(1), e2020RG000708. (e2020RG000708 10.1029/2020RG000708) doi: https://doi.org/10.1029/2020RG000708

Chen, Y.-T., Huang, Y., & Merlis, T. M. (2023). The global patterns of instantaneous CO_2 forcing at the top of the atmosphere and the surface. *Journal of Climate*, *36*(18), 6331 - 6347. doi: https://doi.org/10.1175/JCLI-D-22-0708.1

Flanner, M. G., Huang, X., Chen, X., & Krinner, G. (2018). Climate response to negative greenhouse gas radiative forcing in polar winter. *Geophys. Res. Lett.*, *45*(4), 1997–2004.

Freese, L. M., & Cronin, T. W. (2021). Antarctic radiative and temperature responses to a doubling of CO_2. *Geophys. Res. Lett.*, *48*(17), e2021GL093676.

Fu, Q., & Liou, K. N. (1992). On the correlated k-distribution method for radiative transfer in nonhomogeneous atmospheres. *Journal of Atmospheric Sciences*, *49*(22), 2139 - 2156.

Govindasamy, B., & Caldeira, K. (2000). Geoengineering Earth's radiation balance to mitigate CO_2-induced climate change. *Geophys. Res. Lett.*, *27*, 2141–2144.

Hersbach, H., Bell, B., Berrisford, P., Hirahara, S., Horányi, A., Muñoz-Sabater, J., ... Thépaut, J.-N. (2020). The ERA5 global reanalysis. *Quarterly Journal of the Royal Meteorological Society*, *146*(730), 1999-2049. doi: https://doi.org/10.1002/qj.3803

Huang, Y., & Bani Shahabadi, M. (2014). Why logarithmic? A note on the dependence of radiative forcing on gas concentration. *J. Geophys. Res. Atmospheres*, *119*(24), 13,683-13,689.

Huang, Y., Tan, X., & Xia, Y. (2016). Inhomogeneous radiative forcing of homogeneous greenhouse gases. *J. Geophys. Res.*, *121*, 2780–2789.

Jeevanjee, N., & Fueglistaler, S. (2020). On the cooling-to-space approximation. *J. Atmos. Sci.*, *77*(2), 465 - 478. doi: 10.1175/JAS-D-18-0352.1

Jeevanjee, N., Seeley, J., Paynter, D., & Fueglistaler, S. (2021). An analytical model for spatially varying clear-sky CO_2 forcing. *Journal of Climate*, *34*(23), 9463 - 9480.

Koll, D. D. B., Jeevanjee, N., & Lutsko, N. J. (2023). An analytic model for the clear-sky longwave feedback. *Journal of the Atmospheric Sciences*, *80*(8), 1923 - 1951. doi: https://doi.org/10.1175/JAS-D-22-0178.1

Mlawer, E. J., Taubman, S. J., Brown, P. D., Iacono, M. J., & Clough, S. A. (1997). Radiative transfer for inhomogeneous atmospheres: RRTM, a validated correlated-k model for the longwave. *Journal of Geophysical Research: Atmospheres*, *102*(D14), 16663-16682. doi: https://doi.org/10.1029/97JD00237

Romps, D. M., Seeley, J. T., & Edman, J. P. (2022). Why the forcing from carbon dioxide scales as the logarithm of its concentration. *J. of Climate*, *35*(13), 4027–4047.

Schmithüsen, H., Notholt, J., König-Langlo, G., Lemke, P., & Jung, T. (2015). How increasing CO_2 leads to an increased negative greenhouse effect in Antarctica.

Geophys. Res. Lett., *42*(23), 10,422–10,428.

Sejas, S. A., aylor, P. C., & Cai, M. (2018). Unmasking the negative greenhouse effect over the Antarctic Plateau. *npj Climate and Atmospheric Science*, *1*(17), 2397–3722.

Smith, K. L., Chiodo, G., Previdi, M., & Polvani, L. M. (2018). No surface cooling over antarctica from the negative greenhouse effect associated with instantaneous quadrupling of CO_2 concentrations. *Journal of Climate*, *31*(1), 317 - 323. doi: https://doi.org/10.1175/JCLI-D-17-0418.1

Zhang, M., & Huang, Y. (2014). Radiative forcing of quadrupling CO_2. *J. Climate*, *27*, 2496–2508.